Kinetic and Mechanistic Properties of Biotin Sulfoxide Reductase†

Veronica V. Pollock and Michael J. Barber*

Department of Biochemistry and Molecular Biology, College of Medicine and H. Lee Moffitt Cancer Center and Research Institute, University of South Florida, Tampa, Florida 33612

Received August 4, 2000; Revised Manuscript Received November 10, 2000

ABSTRACT: *Rhodobacter sphaeroides* f. sp. *denitrificans* biotin sulfoxide reductase catalyzes the reduction of *d*-biotin *d*-sulfoxide (BSO) to biotin. Initial rate studies of the homogeneous recombinant enzyme, expressed in *Escherichia coli*, have demonstrated that the purified protein utilizes NADPH as a facile electron donor in the absence of any additional auxiliary proteins. We have previously shown **[**Pollock, V. V., and Barber, M. J. (1997) *J. Biol. Chem. 272*, 3355−3362] that, at pH 8 and in the presence of saturating concentrations of BSO, the enzyme exhibits, a marked preference for NADPH ($k_{cat,app}$ = 500 s^{-1}, $K_{m,app}$ = 269 μM, and $k_{cat,app}/K_{m,app}$ = 1.86 × 10^6 M^{-1} s^{-1}) compared to NADH ($k_{cat,app}$ = 47 s^{-1}, $K_{m,app}$ = 394 μM, and $k_{cat,app}/K_{m,app}$ = 1.19 × 10^5 M^{-1} s^{-1}). Production of biotin using NADPH as the electron donor was confirmed by both the disk biological assay and by reversed-phase HPLC analysis of the reaction products. The purified enzyme also utilized ferricyanide as an artificial electron acceptor, which effectively suppressed biotin sulfoxide reduction and biotin formation. Analysis of the enzyme isolated from tungsten-grown cells yielded decreased reduced methyl viologen:BSO reductase, NADPH:BSO reductase, and NADPH:FR activities, confirming that Mo is required for all activities. Kinetic analyses of substrate inhibition profiles revealed that the enzyme followed a Ping Pong Bi−Bi mechanism with both NADPH and BSO exhibiting double competitive substrate inhibition. Replots of the $1/v$-axes intercepts of the parallel asymptotes obtained at several low concentrations of fixed substrate yielded a K_m for BSO of 714 and 65 μM for NADPH. In contrast, utilizing NADH as an electron donor, the replots yielded a K_m for BSO of 132 μM and 1.25 mM for NADH. Slope replots of data obtained at high concentrations of BSO yielded a K_i for BSO of 6.10 mM and 900 μM for NADPH. Kinetic isotope studies utilizing stereospecifically deuterated NADPD indicated that BSO reductase uses specifically the 4*R*-hydrogen of the nicotinamide ring. Cyanide inhibited NADPH:BSO and NADPH:FR activities in a reversible manner while diethylpyrocarbonate treatment resulted in complete irreversible inactivation of the enzyme concomitant with molybdenum cofactor release, indicating that histidine residues are involved in cofactor-binding.

Biotin sulfoxide reductase (BSO[1] reductase) catalyzes the reduction of *d*-biotin *d*-sulfoxide to *d*-biotin according to the following scheme:

$$d\text{-biotin } d\text{-sulfoxide} + 2e^- + 2H^+ \rightarrow d\text{-biotin} + H_2O$$

The enzyme from *Rhodobacter sphaeroides* has been cloned, sequenced at the genomic DNA level (*1*), and heterologously expressed as a glutathione-S-transferase fusion protein (*2*). Following cleavage of the GST affinity tag, the fusion protein was purified to homogeneity and shown to be a functional MGD (molybdopterin guanine dinucleotide)-containing enzyme that retained $MV^{\bullet+}$:BSOR activity in the absence of any additional redox-active or structural proteins (*2*). A direct spectrophotometric activity assay has been developed using $MV^{\bullet+}$ as the reducing agent which has facilitated examination of the enzyme's oxidizing substrate specificity. BSO reductase uses a variety of substrates such as nicotinamide-*N*-oxide, dimethyl sulfoxide, methionine sulfoxide, and trimethylamine-*N*-oxide, but exhibits a marked preference for BSO (*2*). Its ability to utilize alternative oxidizing substrates suggests that *R. sphaeroides* BSO reductase may play a role as a general protector of the cell from oxidative damage similar to the role proposed for methionine sulfoxide reductase (*3*, *4*) and superoxide dismutase (*5*).

While the structural gene for the *E. coli* BSO reductase (*bis*C) has been cloned and sequenced (*6*), indicating extensive sequence similarities between the *Escherichia coli* and *R. sphaeroides* enzymes, the partially purified *E. coli* BSO reductase has been demonstrated to require two accessory proteins for activity: a small, heat stable, thioredoxin-like moiety, referred to as protein-$(SH)_2$ and an unidentified flavoprotein (*7*). The limited availability of the *E. coli* enzyme coupled with the absence of a direct and convenient spectrophotometric assay has precluded any extensive kinetic and mechanistic examinations.

In this report, we have provided the first demonstration that purified *R. sphaeroides* BSO reductase requires Mo for both NADPH utilization and biotin formation and confirmed that this enzyme is unique among Mo-enzymes since no additional auxiliary proteins or cofactors are required for the

† This work was supported by Grant GM 32696 from NIH.

* To whom correspondence should be addressed. Phone: (813) 974-9702. Fax: (813) 974-7357. E-mail: mbarber@hsc.usf.edu.

10.1021/bi001842d CCC: $20.00
Published on Web 01/09/2001

NADPH-dependent conversion of BSO to biotin. In addition, we have demonstrated for the first time that the enzyme exhibits marked competitive substrate inhibition by both NADPH and BSO, and that the enzyme follows a Ping Pong Bi−Bi mechanism. Utilizing sterospecifically labeled (R)-NADPD and (S)NADPD, a kinetic substrate isotope effect of 2.6 on V_{max}, but not on K_m, was observed only with (R)-NADPD, indicating that BSO reductase specifically utilizes the hydrogen in the *4R*-position of the nicotinamide ring but not the one in the *4S*-position. This kinetic isotope effect further confirms that BSO reductase is unique among Mo enzymes since it utilizes NADPH directly without the involvement of an auxiliary flavoprotein. Further, our work shows that hydride transfer is involved in the reduction of the enzyme by NADPH. Additional inhibition studies have demonstrated that the enzyme is reversibly inactivated by cyanide and irreversibly inactivated by diethyl pyrocarbonate (DEPC), the latter resulting in Mo-cofactor release. The latter results provide the first evidence for the involvement of histidine residues in molybdopterin guanine dinucleotide coordination in BSO reductase.

MATERIALS AND METHODS

Bacterial Strains. E. coli JM 109 was purchased from Promega (Madison, WI). The mutant strain of *E. coli*, ΔMu29 (*E. coli* ΔMu29 is BM 1161 *bis* Mu29Δ that was obtained by Mu insertion into BM1161 followed by the later deletion of Mu which took with it part of the *bisC* gene so it is *bio*$^-$, *bis*$^-$, *thi*$^-$, *str*^{r}) was a generous gift from Dr. Allan Campbell, Stanford University, Stanford, CA.

Chemicals, Enzymes, and Reagents. Factor Xa protease was purchased from Promega while media for bacterial growth was purchased from DIFCO (Detroit, MI). Aprotinin, glucose-6-phosphate dehydrogenase (*Bakers yeast*), alcohol dehydrogenase (*Thermoanaerobium brockii*), antibiotics, biotin, thiamine hydrochloride, DTT, PMSF, reduced glutathione, hydroxylamine, NADPH, $NADP^+$, and basic buffer chemicals were purchased from Sigma Chemical Co. (St. Louis, MO). SDS, acrylamide and bis-acrylamide, protein molecular weight markers, and protein assay solution were purchased from Bio-Rad (Hercules, CA), IPTG was obtained from Research Products International Corp. (Mt. Prospect, IL.). DEPC, 2-propanol-d_8, and D-glucose-1-*d* were purchased from Aldrich Chemical Co. Inc. (Milwaukee, WI). *d*-Biotin *d*-sulfoxide was prepared as described by Pollock and Barber (*1*).

Protein Expression and Purification. For the isolation of recombinant *R. sphaeroides* BSO reductase, transformed *E. coli* JM109 cells were grown overnight and BSO reductase expression induced by addition of IPTG as previously described (*2*) except that for the production of the tungsten-containing enzyme, tungstate was added to the growth medium (to 10 mM final concentration) in place of molybdate 1 h prior to the induction of protein expression with IPTG.

For BSO reductase isolation, the cells were harvested by centrifugation at 3000*g* for 20 min and the cell pellets resuspended in PBS supplemented with DTT (10 mM), aprotinin (0.1 mg/mL), EDTA (1 mM), PMSF (0.1 mM) and either sodium molybdate (1 mM) or sodium tungstate (10 mM). The cells were sonicated on ice and the BSO reductase purified as previously described (*2*) using a combination of glutathione-agarose affinity chromatography, anion-exchange chromatography (Mono-Q) and FPLC gel filtration (Superose 12).

Protein Analysis. Recombinant BSO reductase was examined for purity using both SDS−PAGE and reversed-phase HPLC analysis. Protein samples (1−2 μg of total protein) were analyzed using a 12.5% SDS−PAGE gel (*8*) stained with Coomassie Blue. For reversed-phase HPLC, samples of BSO reductase (30−50 μg) were mixed with an equal volume of 8 M guanidine hydrochloride, acidified with 0.5% acetic acid and chromatographed on a C_4 column (4.6 × 30 mm) using a linear gradient of TFA (0.1%) to TFA (0.1%):acetonitrile (70%). N-Terminal sequencing was performed as described by Pollock and Barber (*1*).

Enzyme Activities. (i) Biotin Analysis Using Reversed-Phase HPLC. The conversion of BSO to biotin was performed in 50 mM Tris-HCl, pH 8, utilizing a NADPH-regenerating system consisting of glucose-6-phosphate and glucose-6-phosphate dehydrogenase in the presence and absence of $K_3Fe(CN)_6$. The reaction products were separated from the proteins using ultrafiltration spin columns (ultrafree MC 5000 MW cutoff, Millipore Corp., Bedford, MA) and were subsequently analyzed by reversed-phase HPLC (Vydac C_{18} column, 4.6 × 250 mm) utilizing a 35 min linear gradient of aqueous TFA (0.05%, pH 2.5) to TFA (0.05%, pH 2.5): acetonitrile (70:30 v/v) at a flow rate of 1 mL/min.

(ii) Disk Microbiological Assay. The disk microbiological assay using *E. coli* ΔMu29 was performed as previously described by Pollock and Barber (*2*). The conversion of BSO to biotin was performed in 250 μL volume containing BSO (1.92 mM), NADPH (40.0 mM), and purified BSO reductase (5−10 μg) in Tris-HCl buffer, pH 8, and was allowed to proceed for 15 min at room temperature. The reaction products were separated from the protein utilizing ultrafiltration spin columns (5000 MW cutoff), diluted 1:1000 with water and aliquots (20 μL) of each reaction product applied to filter disks placed on the top of the minimal glucose plates containing the test organism. Negative control reactions contained BSO and BSO plus NADPH but no enzyme. Positive control reactions contained biotin (1.92 mM, diluted also 1:1000) plus or minus enzyme or biotin plus NADPH. The plates were incubated at 37 °C overnight and inspected for bacterial growth detectable as the formation of red colonies surrounding the filter circles.

[1] Abbreviations: BSO, *d*-biotin *d*-sulfoxide; DMSO, dimethyl sulfoxide; TMANO, trimethylamine-*N*-oxide; MGD, molybdopterin guanine dinucleotide; IPTG, isopropylthio-β-galactoside; *thi*, thiamine hydrochloride; *str*, streptomycin sulfate; amp, ampicillin; bp, base pairs; kb, kilobases; GST, glutathione-*S*-transferase; GST-BSOR, glutathione-*S*-transferase-biotin sulfoxide reductase fusion protein; Da, daltons; SDS, sodium dodecyl sulfate; MW, molecular weight; LB, Luria broth; DTT, dithiothreitol; PBS, phosphate-buffered saline; TE, Tris/EDTA buffer; PMSF, phenylmethanesulfonyl fluoride, TFA, trifluoroacetic acid; DEPC, diethyl pyrocarbonate; $MV^{\bullet+}$, reduced methyl viologen radical cation; $BV^{\bullet+}$, reduced benzyl viologen radical cation; MV:BSOR, reduced methyl viologen:biotin sulfoxide reductase; NADPH:BSOR, NADPH:biotin sulfoxide reductase; NADPH:FR, NADPH:ferricyanide reductase; MSO, methionine sulfoxide; MES, 2-(*N*-morpholino)ethanesulfonic acid; MOPS, 3-(*N*-morpholino)propanesulfonic acid; TRIS, (Tris[hydroxymethyl]amino-methane); CHES, (cyclohexylaminoethane-sulfonic acid); (4*R*)-[^{2}H]NADPH or (R)NADPD, (4*R*)-deuterated-reduced nicotinamide adenine dinucleotide phosphate; and (4*S*)-[^{2}H]NADPH or (S)NADPD, (4*S*)-deuterated reduced nicotinamide adenine dinucleotide phosphate.

Synthesis of (R)NADPD and (S)NADPD. (R)NADPD was synthesized by the method of Jeong (*9*) with some modifications. A total of 35 mg of $NADP^+$ (2.8 mM final concentration), 1.2 mL of 2-propanol-*d*8 (1 M final concentration), and 75 units of alcohol dehydrogenase (*Thermoanaerobium brockii*) were dissolved in 15 mL of 25 mM Tris, pH 9 buffer. The reaction was allowed to proceed at 42 °C, and the formation of (R)NADPD was monitored by following the increase in absorbance at 340 nm. When no further increase in the OD_{340} was observed (about 40 min. after initiating the reaction), the products of the reaction mixture were separated from the enzyme utilizing pressure concentration (10 000 molecular weight cutoff filter). Unreacted 2-propanol and the unwanted product, acetone, were removed by rotary evaporation. The (R)NADPD was precipitated with a ratio of ethanol:(R)NADPD solution of 12:1 following cooling at −20 °C for 20 min and centrifugation at 15 000 rpm for 30 min. The (R)NADPD pellet was solubilized in 1 mL of 50 mM Tris, pH 8, buffer and frozen at −20 °C in aliquots. The A_{260}/A_{340} absorbance ratio of the product was 1.9. To account for any unwanted contaminants in the reaction that could inhibit enzyme activity, NADPH was synthesized from $NADP^+$ using an identical procedure, and both synthesized nucleotides were tested in enzyme assays. (S)NADPD was synthesized by the method of Viola (*10*). The reaction contained 35 mg $NADP^+$ (9.3 mM final concentration) 12 mg of D-glucose-1-*d* (14.7 mM final concentration), 2.56 mL of 83 mM phosphate buffer, pH 8, 1.70 mL of DMSO (40% final concentration), and 50 units of glucose-6-phosphate dehydrogenase. The reaction was allowed to proceed until a maximum absorbance at 340 nm was achieved (1 h at room temperature) and the enzyme removed by filter concentration. The product had an absorbance ratio of A_{260}/A_{340} nm of 1.7. Nondeuterated (S)-NADPH was also synthesized utilizing the same procedure, and both products were used in enzyme activity assays.

Spectrophotometric Assays. BSO reductase (NADPH: BSOR, NADH:BSOR, and NADPH:FR) activities were routinely determined at 25 °C in 84 mM Tris-HCl buffer, pH 8.0, at 340 nm as the oxidation of NADPH (250 μM) or NADH (250 μM) in either the presence of BSO (1.7 mM) or FeCN63- (630 μM) as electron acceptor using 2.5 μg of purified enzyme (31 nM final concentration) in a total volume of 1 mL. NADPH and NADH concentrations were calculated using an ϵ_{340} of 6.22 mM^{-1}. Activities, measured as initial rates, were expressed in units of micromoles of NADPH consumed per minute per nanomole of enzyme. Kinetic parameters were derived from the experimental initial rate data by least-squares fitting to the original hyperbolic rate equation using the software "Enzfitter" (Elsevier Biosoft, Ferguson, MO). Replots of the initial data were performed with the same software. The buffers used for determination of the pH optimum were 73 mM acetic acid, pH 5; 57 mM acetic acid, pH 5.5; 114 mM MES, pH 6; 70 mM MES, pH 6.5; 118 mM MOPS, pH 7; 73 mM MOPS, pH 7.5; 84 mM TRIS, pH 8; 159 mM TRIS, pH 8.5, 184 mM CHES, pH 9; and 116 mM CHES, pH 9.5. The concentrations of the buffers used were calculated such that the ionic strength remained constant ($\mu = 0.05$) over the pH range examined. For the $V_{max,app}$ and $K_{m,app}$ determinations, one substrate remained constant at saturating levels while the other substrate was varied. Due to the marked substrate inhibition by either NADPH or BSO at high concentrations, when substrate inhibition was observed, the concentration of the fixed substrate was decreased to noninhibiting concentrations. Only the linear portions of the double reciprocal plots were utilized for $V_{max,app}$ and $K_{m,app}$ determinations**.** For the kinetic isotope effect studies, both deuterated and nondeuterated, both (S) and (R)NADPH were varied at constant and saturating concentrations of BSO, and in Tris, pH 8, buffer.

Diethylpyrocarbonate Modification. Aliquots of purified BSO reductase (8 μM in 50 mM MES buffer, pH 6) were mixed with DEPC (dissolved in absolute ethanol) to final concentrations of DEPC of 11.5, 4.6, 2.3, and 0.9 mM, respectively. The samples were maintained at 0 °C and NADPH:BSO reductase activities were assessed at varying time intervals following addition of DEPC. NADPH:FR reductase activities were also assessed in the presence of 2.3 and 4.6 mM DEPC at varying times following DEPC addition. Control samples of enzyme were incubated under identical conditions in the absence of DEPC.

Cofactor Analysis of DEPC-Treated BSO Reductase. Aliquots of BSO reductase (8 mM, in 50 mM MES buffer, pH 6) were mixed with DEPC to final concentrations of 23, 46, and 69 mM DEPC, respectively. The samples were maintained at 0 °C for 30 min following each DEPC addition to allow the reaction to proceed to completion. For the enzyme samples treated with elevated DEPC concentrations (46 and 69 mM final), the DEPC was added in two and three separate aliquots respectively, each followed by a 30 min incubation. Control enzyme samples were treated in an identical manner except for the omission of DEPC. Following modification, enzyme samples were dialyzed overnight in 50 mM Tris buffer, pH 7, denatured with 1% SDS for 30 min followed by boiling for 20 min. The SDS was precipitated with KCl (0.25 M final concentration), and the cofactor separated from the protein utilizing ultra filtration spin columns ("ultrafree-MC" 5000 MW cutoff). The amount of cofactor contained in each sample was determined by fluorescence spectroscopy using an excitation wavelength of 370 nm.

Cyanide Modification. NADPH:BSOR and NADPH:FR activities were recorded in the presence of increasing concentrations (up to 10 mM) of KCN. In addition, purified enzyme was incubated with KCN (10 mM final concentration) prior to assaying for activity. To examine whether cyanide inactivation was reversible, the enzyme was dialyzed to remove the cyanide followed by activity determinations.

RESULTS

BSO Reductase Purity. To ensure that the kinetic properties of the enzyme were not influenced by contaminating proteins and were independent of any accessory proteins that have been indicated to be required for the corresponding *E. coli* enzyme (*7*), recombinant *R. sphaeroides* BSO reductase was purified to homogeneity and analyzed both by SDS−PAGE and reversed-phase HPLC. As shown in Figure 1, following anion-exchange and gel filtration chromatography of the Factor Xa-cleaved BSO reductase, the purified enzyme exhibited a single band of approximately 80 kDa on SDS−PAGE (Figure 1, lane A) and eluted as a single peak from the reversed-phase HPLC column with a retention time of 40.5 min (data not shown). Direct N-terminal sequencing of

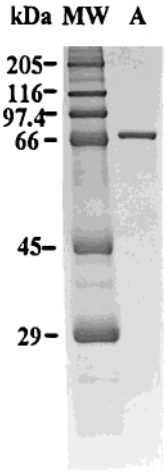

FIGURE 1: SDS−PAGE analysis of recombinant *R. sphaeroides* BSO reductase. Purified recombinant BSO reductase (2 μg, Lane A) was analyzed on a 12.5% SDS PAGE gel. Lane MW represents standard molecular weight markers.

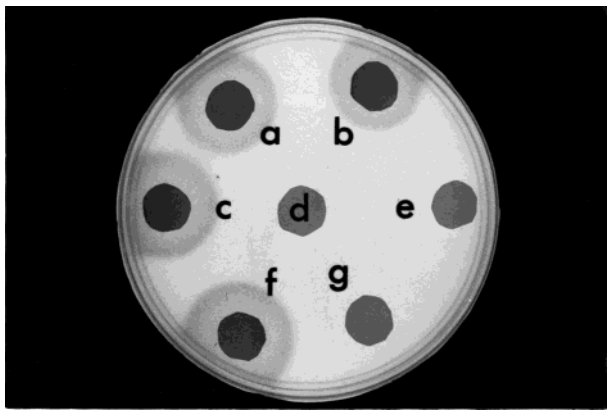

FIGURE 2: Microbiological disk assay for BSO reductase activity. The disk biological assay was utilized to confirm the presence of biotin as a product of BSO reductase activity. The reactions were performed as described in the Materials and Methods with *E. coli* ΔMu29 as the test organism. Diluted aliquots (20 μL each) of the reaction products that had been separated from the protein by ultrafiltration were applied to the nitrocellulose disks. Disk a: biotin, NADPH, BSO reductase, and buffer. Disk b: BSO, NADPH, buffer, and BSO reductase. Disk c: biotin, NADPH, and buffer. Disk d: NADPH and buffer. Disk e: BSO, NADPH, and buffer. Disk f: biotin and buffer. Disk g: BSO and buffer. The test organism grew only around the filters containing biotin or the product of the reaction of NADPH with BSO in the presence of BSO reductase.

the HPLC-isolated enzyme yielded the single amino acid sequence YPITRVPH, indicating correct cleavage of the BSO reductase from the GST expression tag.

BSO Reductase Activities. (i) Disk Microbiological Assay. To confirm the identity of the NADPH:BSO reductase-catalyzed reaction product eluting at 18.7 min from the reversed-phase HPLC column, we utilized the reaction product in the disk microbiological assay, as shown in Figure 2. *E. coli* ΔMu29 mutants were unable to grow utilizing either BSO and buffer (disk g) or BSO, NADPH, and buffer (disk e), respectively. However, growth of the mutants was evident, visible as red halos surrounding the disks, in the presence of biotin and buffer (disk f), biotin, NADPH, and buffer (disk c), biotin, NADPH, BSO reductase, and buffer (disk a), as well as the products of the reaction between BSO and NADPH catalyzed by BSO reductase (disk b). Thus, growth of the test organism was sustained only in the presence of authentic biotin or the product of the NADPH:BSOR reaction. These results confirmed the product's identity and indicated that NADPH functioned as a facile donor of reducing equivalents.

Table 1: Comparison of the Specific Activities of BSO Reductase Expressed in the Presence of Mo or W

	BSO reductase specific activity[a]	
activity	MoO_4^{2-}-grown cells	WO_4^{2-}-grown cells
NADPH:BSOR	30.0	14.8
NADPH:FR	1.70	0.69
MV:BSOR	0.90	0.43

[a] Specific activities were determined in 50 mM Tris buffer, pH 8, and are expressed as μmol of NADPH consumed or BSO formed/min/nmol BSO reductase.

(ii) HPLC Analysis. The ability of the purified BSO reductase to convert BSO to biotin, utilizing NADPH as an electron donor in the absence of any accessory proteins, was initially examined using reversed-phase HPLC analysis of the reaction products utilizing a NADPH regenerating system and in the presence and absence of ferricyanide. BSO was converted to biotin utilizing NADPH only in the absence of ferricyanide as shown by the appearance of a biotin peak eluting at 18.7 min (data not shown).

Analysis of Tungsten-Containing BSO Reductase. Incorporation of tungsten has been used as a convenient method of assessing the requirement for Mo in the functionality of putative Mo-containing enzymes (*12*). Tungsten-substituted molybdoenzymes are generally inactive owing to the lower reduction potential of the W site relative to the Mo site (*12*). To confirm that both BSO reductase-catalyzed activities (NADPH:BSOR and NADPH:FR) required Mo, the specific activities of the enzyme isolated from *E. coli* grown in the presence of Mo (*E. coli* cannot grow initially in the absence of Mo**)**, but expressed in the presence of 10 mM tungsten were determined and are shown in Table 1. For the enzyme expressed in the presence of tungstate, the NADPH:BSOR, NADPH:FR, and MV:BSOR specific activities were all decreased to approximately 50% of the activity of the enzyme expressed in the presence of molybdate, indicating that Mo was required for both NADPH oxidation as well as BSO reduction. The 50% loss of activity indicates that about 50% of the expressed protein incorporated tungsten instead of Mo.

Kinetic Properties. The direct demonstration of the ability of NADPH to function as a facile electron donor for BSO reductase activity in the absence of any accessory proteins provided a direct and convenient spectrophotometric assay with which to examine for the first time a variety of kinetic and mechanistic properties of the enzyme. To facilitate detailed kinetic studies, we examined the pH dependence of both full (NADPH:BSOR) and partial (NADPH:FR) enzyme activities. The NADPH:BSOR and NADPH:FR activities as a function of pH, under conditions of constant ionic strength ($\mu = 0.05$), are shown in Figure 3. Initial rate kinetic studies of NADPH:BSOR activity performed at various pH's within the range 5−9.5 indicated significant substrate inhibition by both NADPH and BSO at concentrations that varied with the applied pH. Thus, NADPH concentrations greater than 60 and 300 μM were observed to be inhibitory at pH 5 and 9.5, respectively, while BSO concentrations greater than 500

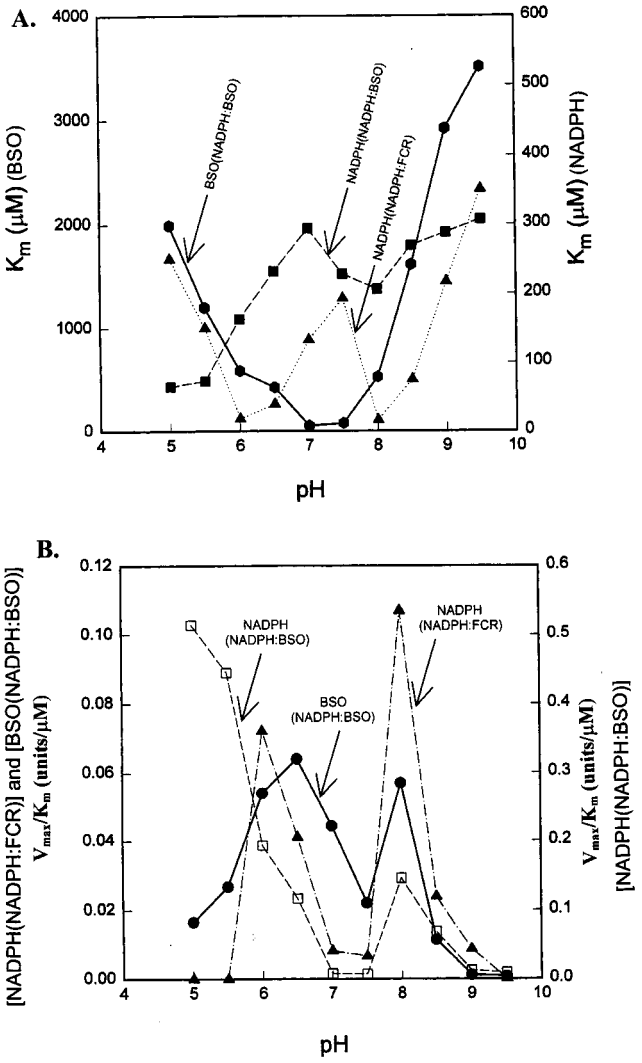

FIGURE 3: BSO reductase pH optimum profiles. The reactions were performed in 1 mL total volume at fixed concentrations of one substrate while varying the second substrate and using 2.5 μg of purified BSO reductase, in buffers described in the Materials and Methods. Activities were monitored at 340 or 375 nm and were expressed as activity units (μmol of NADPH consumed/min/nmol of enzyme). The data were plotted as K_m (μM) versus pH, Figure 3A, and V_{max}/K_m (units/μM) versus pH, Figure 3B. In determining the V_{max} and K_m for BSO, to avoid substrate inhibition by BSO, the concentration of BSO was varied between 19 and 960 μM at pH's 5.0, 5.5, 6.0, and 6.5; between 19 and 480 μM at pH's 7.0 and 7.5; and between 96 and 1920 μM at pH's 8.0, 8.5, 9.0, and 9.5. To avoid substrate inhibition by NADPH, its concentration was kept fixed at 120 μM at pH's 5.0 and 5.5; at 300 μM at pH 6.0 and at 630 μM at pH's 6.5, 7.0, 7.5, 8.0, 8.5, 9.0, and 9.5. In determining the V_{max} and K_m for NADPH, to avoid substrate inhibition by NADPH, the concentration of NADPH was varied between 10 and 51 μM at pH 5.0; between 25 and 100 μM at pH 5.5; between 17 an 200 μM at pH 6.0 and 6.5; between 50 and 250 μM at pH's 7.0, 7.5, 8.0, 8.5, and 9.0; and between 90 and 250 μm at pH 9.5. To avoid substrate inhibition by BSO, its concentration was kept constant at 1920 μM at pH's 5.0, 5.5, 6.0, 6.5, 8.0, 8.5, 9.0, and 9.5; at 480 μM at pH 7 and at 960 μM at pH 7.5. In determining the V_{max} and K_m for NADPH, in the NADPH:FR reaction, to avoid substrate inhibition by NADPH, its concentration was varied between 35 and 250 μM at pH's 5.0 and 9.0; between 25 and 180 μM at pH's 5.5, 7.0, and 7.5; between 6.0 and 110 μM at pH's 6.0, 6.5, and 8.0; between 20 and 150 μM at pH 8.5; and between 40 and 250 μM at pH's 9.0 and 9.5. The ferricyanide concentration was maintained constant at 630 μM except for pH's 8.0 and 8.5 where it was increased to 1 mM.

μM and 2 mM were observed to be inhibitory at pH 7 and 9.5, respectively. Thus, for the initial rate experiments, the fixed substrates were maintained at noninhibitory levels and data points corresponding to only the linear portion of the Lineweaver−Burk plots obtained for the variable substrate were used for $V_{max,app}$ and $K_{m,app}$ determinations. Control experiments were performed to confirm that the pH extremes did not inactivate the enzyme during the assay period or did not result in substrate degradation.

The dependence of $K_{m,app}$ for both BSO and NADPH as a function of pH is shown in Figure 3A, and values obtained for the specificity constant, $V_{max,app}/K_{m,app}$, for the NADPH:BSOR activity as either a function of NADPH or BSO at various pHs are shown in Figure 3B, together with the results obtained for the NADPH:FR activity. Specific values obtained at each pH are given in Table 2.

For the NADPH:BSOR reaction, the minimum $K_{m,app}$ for BSO, corresponding to 51 μM, was determined at pH 7, while in contrast the maximum $K_{m,app}$ was determined to be 3.5 mM at pH 9.5. For NADPH, the minimum $K_{m,app}$ was determined to be 64 μM at pH 5 and the maximum $K_{m,app}$ was determined to be 307 μM at pH 9.5. In contrast, maximum and minimum turnover numbers for the NADPH:BSOR activity were determined to be 552 s^{-1} ($V_{max,app}$ = 33.1 units) at pH 5 and 28.3 s^{-1} ($V_{max,app}$ = 1.7 units) at pH 7.5, respectively. Optimum values for the specificity constant for NADPH and BSO were obtained at pH 5 ($V_{max,app}/K_{m,app}$ = 5.1 × 10^{-1} units/μM) and pH 6.5 ($V_{max,app}/K_{m,app}$ = 64.1 × 10^{-3} units/μM), respectively.

Values for the specificity constant as a function of pH for the NADPH:FR partial activity were also determined in order to obtain information about the binding of NADPH and the specific activity of the enzyme in the absence of the second physiological substrate BSO. Ferricyanide acts as an artificial electron acceptor, which does not require a specific binding site and does not exhibit the inhibitory effects of BSO on BSOR activity. The $K_{m,app}$'s for NADPH, in the absence of BSO, were significantly lower than in the presence of BSO (the inhibitory effect of BSO was absent), and exhibited two minima, one at pH 6 and one at pH 8, suggesting that in the absence of BSO, NADPH may have two binding sites one of which is preferentially utilized at low pH and the other at high pH. In the presence of BSO, the $K_{m,app}$ for NADPH reached a minimal value at low pH, suggesting that NADPH binding was preferred under weakly acidic conditions in the presence of BSO. Minimum and maximum values obtained for the $K_{m,app}$ for NADPH, in the NADPH:FR reaction, corresponded to 16 μM at pH 8 and 350 μM at pH 9.5 whereas the maximum and minimum turnover numbers were obtained at pH 9 ($V_{max,app}$ = 1.9 units) and pH 5 ($V_{max,app}$ = 0.01 units), respectively (Table 2).

The biphasic nature of the pH dependence of the specificity constants for both BSO and NADPH in the NADPH:BSOR and NADPH:FR reactions, respectively, may indicate that both an acidic and a basic residue are involved in catalysis. However, the values for the specificity constant for NADPH in the NADPH:BSOR reaction indicate that the reaction is more favorable at low pH. Since the initial rate data suggests that the kinetic mechanism of BSO reductase is a Ping Pong Bi−Bi mechanism, one pH optimum may favor the reduction of the enzyme by NADPH via a hydride transfer mechanism while the other may favor the reduction of BSO, or

Table 2: pH Dependence of $K_{m,app}$ and $V_{max,app}$ for BSO and NADPH Utilizing NADPH:BSOR and NADPH:FR Activities[a]

	BSO			NADPH			NADPH (FR reaction)		
pH	V_{max} (units)	K_m (μM)	V_{max}/K_m (units/μM)	V_{max} (units)	K_m (μM)	V_{max}/K'_m (units/μM)	V_{max} (units)	K_m (μM)	V_{max}/K_m (units/μM)
5.0	33.1	1990	16.6×10^{-3}	33.1	64	5.1×10^{-1}	0.01	250	4.0×10^{-5}
5.5	32.2	1200	26.8×10^{-3}	32.4	72	4.5×10^{-1}	0.12	150	8.0×10^{-5}
6.0	31.4	583	53.9×10^{-3}	31.5	163	1.9×10^{-1}	1.29	18	7.2×10^{-2}
6.5	27.1	423	64.1×10^{-3}	27.1	232	1.2×10^{-1}	1.60	39	4.1×10^{-2}
7.0	2.3	51	44.3×10^{-3}	2.3	294	7.8×10^{-3}	1.10	133	8.3×10^{-3}
7.5	1.7	74	22.1×10^{-3}	1.7	228	7.2×10^{-3}	1.30	193	6.7×10^{-3}
8.0	29.8	524	56.9×10^{-3}	30.0	206	1.5×10^{-1}	1.70	16	1.1×10^{-1}
8.5	18.5	1610	11.5×10^{-3}	18.6	269	6.9×10^{-2}	1.80	75	2.4×10^{-2}
9.0	3.6	2920	1.2×10^{-3}	3.6	288	1.3×10^{-2}	1.90	217	8.8×10^{-3}
9.5	2.8	3510	0.80×10^{-3}	2.9	307	9.0×10^{-3}	0.03	350	8.6×10^{-5}

[a] 1 unit = 1 μmol of NADPH consumed /min/nmol BSOR.

alternative oxidizing substrate, by the reduced enzyme. Support for this rationale is that the K_m for NADPH is relatively low at acidic pH (pH 5), whereas the K_m for BSO is low at a higher pH (pH 7). In addition, the specificity constant is relatively high for NADPH at low pH (pH 5) and that for BSO is biphasic (high at pH 6.5 and 8). However, the data analysis is complicated by substrate inhibition effects, exhibited by both substrates, that are both concentration and pH dependent.

Mechanistic Analysis. To examine the kinetic mechanism of BSO reductase, maximal rates for NADPH:BSOR activity were determined at various concentrations of each substrate, at three different, fixed and uninhibiting concentrations of the second substrate. The results, shown in Figure 4A, are plotted as the reciprocal of specific maximal activity versus the reciprocal of the varied substrate concentration. Points at which the varied substrate inhibited the activity were omitted so that only the linear portion of the plots is shown.

With increasing concentrations of each of the fixed substrates, both the $V_{max,app}$'s and $K_{m,app}$'s for the varied substrate increased, yielding Lineweaver−Burk plots consisting of a series of parallel lines (Figure 4A left and right panels) and indicating that the enzyme follows a Ping Pong Bi−Bi mechanism (*13*).

The K_m's for BSO and NADPH were obtained from replots of the 1/v-axis intercepts of the parallel asymptotes obtained at three low concentrations of the fixed substrate (from Figure 4A). These replots are illustrated in Figure 4B and values obtained are shown in Table 3.

Similar experiments were performed with NADH as the reducing substrate for BSO reductase yielding a series of parallel lines at fixed concentrations of BSO (corresponding to 120, 240, and 480 μM, respectively) and varying NADH concentrations, as well as at fixed concentrations of NADH (corresponding to 170, 209, and 276 μM, respectively) and varying BSO concentrations (data not shown). Replots performed as for the NADPH data yielded the K_m values for NADH and BSO given in Table 3.

To examine the mechanism of substrate inhibition, one substrate (BSO) was maintained at several fixed and inhibiting concentrations while the concentration of the second substrate (NADPH) was varied. As shown in Figure 5A (lines B, C, D, and E), with increasing inhibitory concentrations of the fixed substrate, the slopes of the Lineweaver−Burk plots increased. At high inhibitory levels of the fixed substrate (lines C, D, and E), the lines converged to intersect at the same point on the y-axis, indicating that at high inhibitory concentrations of the fixed substrate, $V_{max,app}$ was unchanged and only the $K_{m,app}$ was affected. This pattern is indicative of competitive substrate inhibition of enzyme activity. In addition, substrate inhibition by the varied substrate was also observed since the Lineweaver−Burk plots indicated a lower velocity than $V_{max,app}$ at high, inhibitory concentrations of the varied substrate. As the fixed BSO concentration increased, inhibition by NADPH was only observed at increasingly elevated concentrations of NADPH. The double competitive substrate inhibition pattern suggests that the reactants give rise to competitive substrate inhibition by combining with an improper stable enzyme form (*13*). Supporting evidence for this conclusion comes from resonance Raman studies performed on BSO reductase indicating that, unlike DMSO reductase, BSO reductase cannot be reduced to the Mo(IV) state by the product, biotin, or alternative products such as DMSO, even though these products bind to the enzyme (*14*) and probably form an improper stable enzyme form resulting in product inhibition. These data strongly indicate that double competitive substrate inhibition in a Ping Pong mechanism (*15*) occurs for *R. sphaeroides* BSO reductase.

The dissociation constant for BSO from the dead end complex, K_{iBSO} was obtained from slope replots of the data obtained at high and inhibitory concentrations of the fixed substrate, BSO. The replot is illustrated in Figure 5B and yielded a K_i for BSO of 6.1 mM. Substituting this value in the velocity equation (shown below) for double competitive substrate inhibition in a Ping Pong mechanism (*16*) yielded a K_i for NADPH of 900 μM.

$$v/V_{max} = [[BSO][NADPH]]/ [K_{m,NADPH}[BSO](1 + [BSO]/K_{i,BSO}) + K_{m,BSO}[NADPH] (1 + [NADPH]/K_{i,NADPH}) + [NADPH][BSO]] \quad (1)$$

Substituting individual data values into this equation in addition to the K_m values for BSO and NADPH obtained from replots of the data from the parallel lines yielded K_i's for BSO and NADPH of 6.38 mM and 911 μM, respectively, in good agreement with the values obtained from Figure 5B.

Kinetic Deuterium Isotope Effect on BSO Reductase Activity. To further confirm that BSO reductase utilizes NADPH as a direct electron donor substrate, and to determine whether this enzyme utilizes stereospecifically the *4R*- or *4S*-hydrogen of the nicotinamide ring, (*4R*)NADPD and (*4S*)-

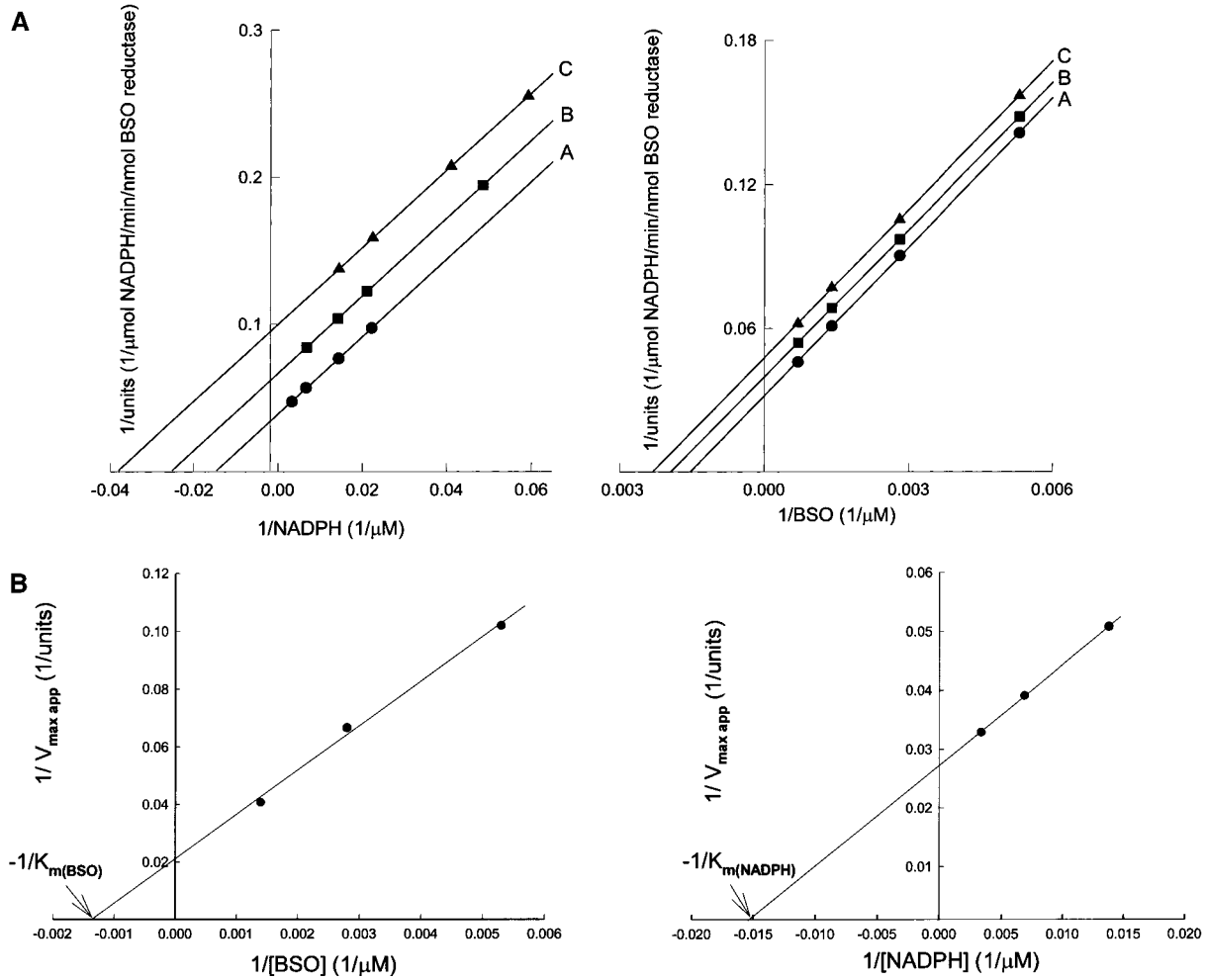

FIGURE 4: BSO reductase kinetic mechanism. (double reciprocal plots). (A) For this experiment, one substrate was varied while the second was maintained constant at three, fixed, uninhibitory concentrations. The rates were measured at each substrate concentration and plotted as the reciprocal of V_{max}, measured in activity units (μmol of NADPH consumed/min/nmol enzyme) versus the reciprocal of the varied substrate concentration (1/μM). The reactions were performed in 1 mL of Tris buffer, pH 8, and in the presence of 2.5 μg of purified BSO reductase. (Right panel) The concentration of NADPH was maintained constant at either 290 μM (A), 145 μM (B), or 72.3 μM (C), while the concentration of BSO was varied between 200 μM and 1.5 mM. (Left panel) The concentration of BSO was maintained constant at either 720 μM (A), 360 μM (B), or 187.5 μM (C), while the NADPH concentration was varied between 45 and 300 μM (A), 20 and 150 μM (B), and 16 and 70 μM (C). (B) The K_m for BSO (left panel) and that for NADPH (right panel) were obtained from replots of the 1/v-axis intercepts of the parallel asymptotes obtained at the three low concentrations of the fixed substrate and illustrated in Figure 4A, respectively.

Table 3: K_m Values for NADPH, BSO, and NADH[a]

	NADPH:BSO (μM)	NADH:BSO (μM)
$K_{m,BSO}$	714	132
$K_{m,NADPH}$	64.5	
$K_{m,NADH}$		1250

[a] K_m values were obtained from replots of the reciprocals of V_{max} of the parallel lines versus the reciprocals of the fixed substrate concentrations.

NADPD were synthesized and the enzyme activities were determined and compared to those obtained utilizing NADPH. As shown in Figure 6, in the presence of (*4R*)-NADPD, V_{max} was reduced 2.6-fold while no effect was observed on the K_m when compared with the data obtained in the presence of NADPH. There was no kinetic isotope effect observed with (*4S*)NADPD. These data suggest that BSO reductase utilizes only the *4R*-hydrogen of the nicotinamide ring, and that this is a primary isotope effect requiring the breakage of the *4R*-hydrogen−carbon bond.

Cyanide Inhibition. Cyanide inhibition has frequently been used to examine the nature of the thiol ligands at the active site of molybdenum-containing enzymes (*17*). The inhibition of BSO reductase activity by cyanide is shown in Figure 7. Increasing concentrations of cyanide were observed to significantly decrease the NADPH:BSOR activity, with 10 mM KCN reducing the activity to only 7% of the initial value. However, removal of the cyanide from the enzyme by dialysis resulted in restoration of the original level of activity indicating that cyanide inhibition was reversible and suggesting the absence of any cyanolysable sulfur ligands (*18*), a result which is consistent with the observation that, like DMSO reductase, BSO reductase has a free oxo ligand and not a free sulfur ligand at its active site (*19*). Very similar results were observed for the effects of cyanide on NADPH:FR activity.

Diethylpyrocarbonate Modification. Three histidine residues have recently been shown to be involved in binding the MGD cofactors in *R. sphaeroides* DMSO reductase (*20*). These histidine residues are also conserved in BSO reductase

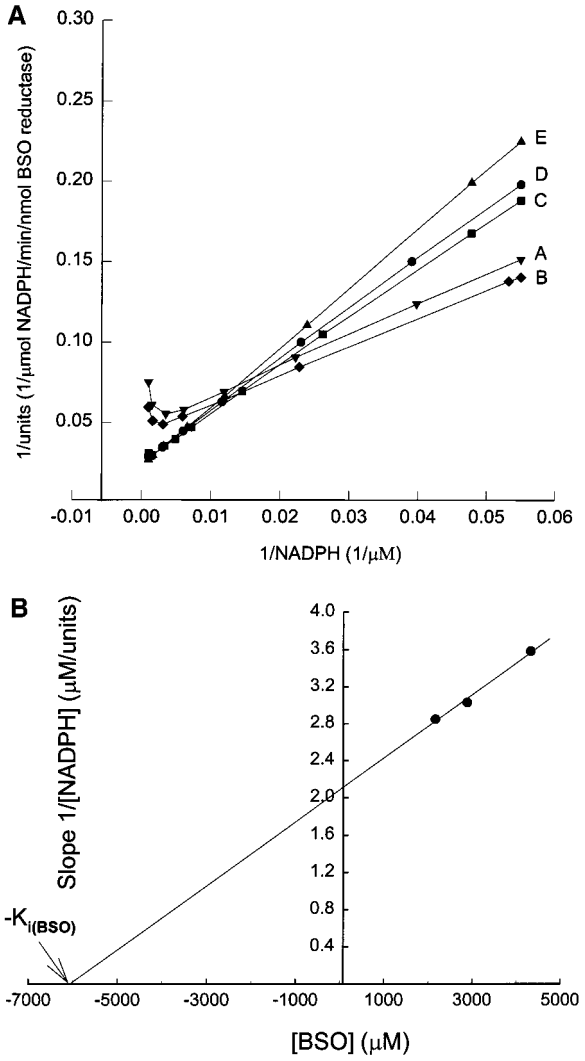

FIGURE 5: BSO reductase substrate inhibition. (A) The disappearance of NADPH was monitored at 375 nm to allow the use of higher concentrations of NADPH, concentrations at which this substrate was also inhibiting. Rates were measured in Tris buffer, pH 8, using 2.5 μg of BSO reductase, and various NADPH concentrations while maintaining the BSO substrate concentrations at four fixed inhibitory levels of 1440 (B), 2160 (C), 2880 (D), and 4320 μM (E), respectively. In addition one fixed uninhibitory BSO concentration of 1080 μM (A) was also used for comparison. Data points where the concentration of the variable substrate NADPH was inhibiting were also included in this plot to illustrate inhibition by both substrates. The data were plotted as the reciprocal of the specific activity (units) versus the reciprocal of the variable substrate concentration. (B) Slope replots of data (illustrated in panel A) obtained at three high concentration of fixed substrate, 2160, 2880, and 4320 μM BSO.

(*21*). To examine the effects of histidine modification on the properties of BSO reductase, the enzyme was modified with DEPC, a reagent with a high specificity for His residues in the pH range of 5.5−7.5 (*22*). As shown in Figure 8 (left panel), addition of increasing amounts of DEPC to BSO reductase resulted in complete inactivation of both the NADPH:BSOR and NADPH:FR activities. In the presence of 2.3 mM DEPC, inactivation was complete within 50 min while increasing the DEPC concentration to 11.5 mM reduced the inactivation time to 10 min. Neither NADPH:BSOR nor NADPH:FR activity was restored following treatment of the DEPC-modified enzyme with either high pH Tris buffer or hydroxylamine (*22*).

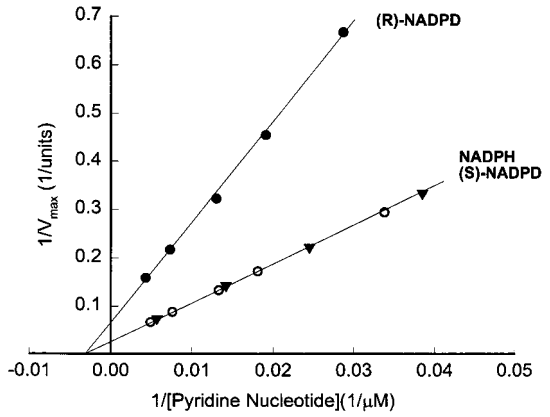

FIGURE 6: Steady-state kinetic deuterium isotope effects on BSO reductase using deuterated NADPH. NADPH consumption for BSO production was monitored at 340 nm as described in the Materials and Methods. The data obtained from the kinetic assays was plotted as Lineweaver−Burk plots [double reciprocal plots of V_{max} (activity units in μmol of pyridine nucleotide consumed/min/nmol of BSO reductase)] versus pyridine nucleotide concentrations utilizing (R)-NADPD (●), NADPH (○), and (S)NADPD (▼). Reactions were performed in 1 mL volume of 50 mM Tris buffer, pH 8, containing BSO 1.9 mM, BSO reductase 11.3 nM, and varying concentrations of the pyridine nucleotides, respectively.

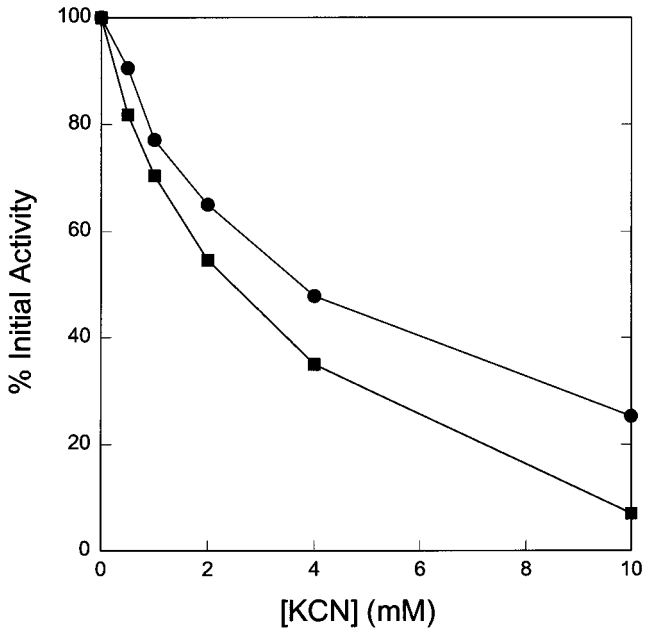

FIGURE 7: Inhibition of BSO reductase by cyanide. NADPH:BSOR (●) and NADPH:FR (■) activities were determined in the presence of increasing concentrations (0.0, 0.5, 1.0, 2.0, 4.0, and 10.0 mM) of KCN, and the results plotted as the percent activity remaining in the presence of the specified amount of KCN versus concentration of KCN. 50% of the NADPH:BSOR activity was lost in the presence of 2.4 mM KCN.

Since DEPC-inactivated BSO reductase irreversibly, we examined whether histidine modification resulted in the release of the MGD cofactor from the enzyme. Incubation of BSO reductase with increasing concentrations of DEPC resulted in increased cofactor release as demonstrated by the fluorescence analysis, shown in Figure 8 (right panel) of cofactor isolated from native and DEPC-inactivated enzyme. The observation that complete inactivation of BSO reductase occurred at a DEPC concentration (2.3 mM) substantially lower than that resulting in liberation of 62% of the enzyme's cofactor (23 mM) suggests that complete modification of

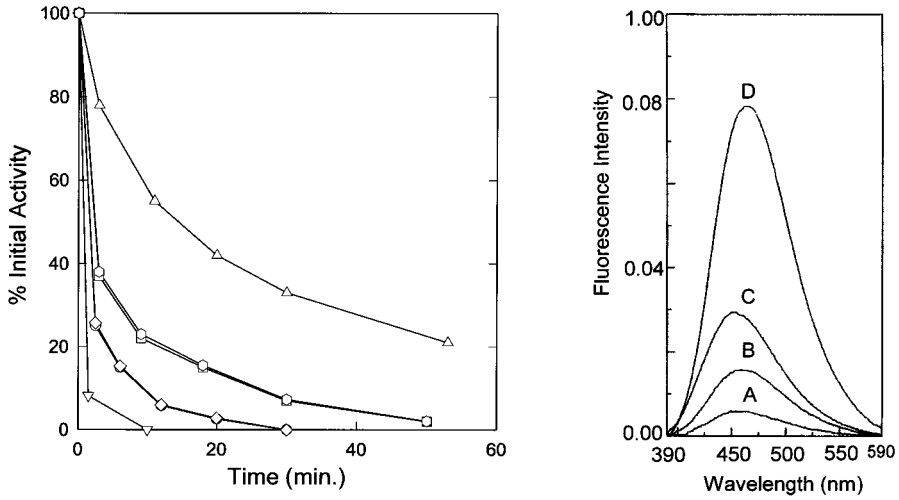

FIGURE 8: DEPC inactivation of BSO reductase and cofactor analysis of the inactivated enzyme. (Left panel) BSO reductase was treated with DEPC as described in the Materials and Methods. The percent remaining NADPH:BSOR activity was plotted versus time following DEPC addition. The 100% activity corresponds to the activity of BSO reductase treated only with the same amount of ethanol as contained in the DEPC treated samples (1%). BSO reductase (100 μL of 8 μM) was treated with final DEPC concentrations of 0.9 mM (△), of 2.3 mM (□), of 4.6 mM (○), and of 11.5 mM (▽). NADPH:FR activity was plotted for samples treated with 2.3 mM DEPC (○) and 4.6 mM DEPC (◇), respectively. (Right panel) BSO reductase was treated with DEPC, and cofactor was isolated from untreated as well as DEPC-treated enzyme as described in the Materials and Methods. The fluorescence emission spectra of cofactor isolated from DEPC-treated and untreated enzyme were recorded using an excitation wavelength of 370 nm. Fluorescence spectra of cofactor isolated from untreated enzyme (D) and from BSO reductase treated with 23.0 mM (C), 46.0 mM (B), and 69.0 mM (A) DEPC, respectively, are shown.

histidine residues is not required for abolition of NADPH:BSOR and NADPH:FR activity but may be required for extensive cofactor dissociation. These results provide the first indication that histidine residues are essential for BSO reductase activity and are involved in cofactor binding in a manner similar to DMSO reductase.

DISCUSSION

The preceding results demonstrate that BSO reductase from *R. sphaeroides* is able to utilize NADPH and, to a lesser degree, NADH directly as electron donors for the conversion of *d*-biotin sulfoxide to *d*-biotin in the absence of any accessory proteins. In addition, the enzyme was found to use only the *4R*-hydrogen from the nicotinamide ring of NADPH. Thus, BSO reductase is the only known Mo-enzyme in which NADPH serves as a direct electron donor to the Mo center.[2] In addition, the enzyme has been shown to exhibit a NADPH:FR partial activity while chemical modification studies have indicated that histidine residues are essential for activity and cofactor binding. Kinetic mechanistic studies have demonstrated for the first time that this enzyme follows a Ping Pong Bi−Bi mechanism and exhibits competitive substrate inhibition by both its substrates, NADPH and BSO.

Previous work on BSO reductase has been limited to the partial purification of the enzyme from *E. coli* to an undetermined purity (*7*) and partial characterization of this enzyme in the presence of added lysate owing to the requirement for auxiliary proteins for activity. We have expressed BSO reductase from *R. sphaeroides* in *E. coli*, and purified it to homogeneity. In contrast to the *E. coli* enzyme, we have shown that BSO reductase from *R. sphaeroides* does not require any auxiliary proteins for activity and that the enzyme contained only MGD as cofactor. We have also shown that the enzyme could directly utilize pyridine nucleotides as electron donors as well as reduced methyl viologen or reduced benzyl viologen as artificial electron donors and that the activity could be monitored directly, as the disappearance of NADPH at 340 nm (*2*). The previous development of a spectrophotometric assay (*2*) has facilitated a more detailed kinetic analysis of BSO reductase.

To further characterize *R. sphaeroides* BSO reductase, we have demonstrated by two alternate methods, reversed-phase HPLC and the disk microbiological assay, that the product of the reaction catalyzed by BSO reductase utilizing NADPH as an electron donor is biotin. The *E. coli* enzyme has been shown using the disk biological assay to have a nonphysiological pH optimum of 9.5 and an apparent K_m for BSO of 5.7 μM at pH 9.5 (*7*). In contrast, we have shown using the spectrophotometric assay that BSO reductase from *R. sphaeroides* appears to have two pH optima (pH 6 and 8), as illustrated in the specificity constants obtained for the NADPH:BSOR reaction. This may suggest that the enzyme undergoes a conformational change which is pH dependent and which favors optimum catalysis at two pH's or that NADPH has two binding sites, one which is preferred at low pH and the other at high pH. In the presence of BSO, NADPH binding appears to be more effective at lower pH. BSO reductase from *R. sphaeroides* also appears to have a much higher $K_{m,app}$ for BSO, corresponding to 583 and 524 μM at pH 6 and pH 8, respectively.

To test whether the high K_m values obtained for BSO and NADPH were potentially due to the fact that, in vivo, other auxiliary proteins may be involved in catalysis, we have determined the enzyme's activity in the presence and absence of added whole cell lysate from both *E. coli* and *R. sphaeroides*, respectively. In the presence of added lysate which had not been dialyzed, the activity of BSO reductase decreased, presumably due to the presence of small inhibitory molecules such as FAD and $NADP^+$ (data not shown). In

[2] The term "Mo-pterin center" is used to refer to the complex of Mo, molybdopterin, and associated protein ligands to Mo.

the presence of dialyzed lysate, the activity was unchanged from values obtained in the absence of added lysate, suggesting no stimulation by exogenous proteins. From these results, it is apparent that, in contrast to the *E. coli* enzyme, BSO reductase from *R. sphaeroides* requires no auxiliary proteins for either NADPH:BSOR or NADPH:FR activity.

Previously, utilizing $MV^{\bullet+}$ as an artificial electron donor, the K_m for BSO was determined to be only 15 μM, at pH 8 (*2*), while utilizing ferricyanide as an artificial electron acceptor, the K_m for NADPH has been determined to be 16 μM, at pH 8. The increased K_m obtained for each of the substrates in the presence of the physiological second substrate, when compared with the K_m obtained in the presence of an artificial electron donor or acceptor [$MV^{\bullet+}$, and $Fe(CN)_6^{3-}$], can be explained by the marked competitive inhibition exhibited by each of the physiological substrates toward the second physiological substrate. We have shown for the first time that BSO reductase follows a Ping Pong Bi−Bi mechanism with marked competitive inhibition exhibited by each substrate toward the second substrate. Due to the nature of the Ping Pong mechanism (*13*), when the fixed substrate concentration is lowered, both the $K_{m,app}$ and the $V_{max,app}$ for the varied substrate decrease so that the slopes of the Lineweaver−Burk plots remain constant. This indicates that at low, physiological concentrations of each substrate, the K_m for the other substrate is also low, and probably within a physiological range, while the turnover number of the enzyme is still high. The marked competitive inhibition by both substrates aided interpretation of the nature of the high $K_{m,app}$ values obtained for each substrate, at each pH optimum, under saturating conditions of the second substrate. Replots of the $1/v$-axis intercepts of the parallel asymptotes obtained at low concentrations of the fixed substrate indicated that the actual K_m for BSO was 714 μM and that for NADPH was 65 μM, a lower value than initially obtained under inhibitory conditions of BSO (*2*). Similar plots performed with NADH as an electron donor yielded a K_m for BSO of 132 μM and that for NADH of 1250 μM, at pH 8, and indicated that double competitive inhibition also occurred with NADH. Both the high K_m and the low $V_{max,app}$ obtained for NADH suggest that NADPH is the physiological electron donor for BSO reductase.

In contrast to the NADPH:BSOR reaction, where substrate inhibition by BSO was observed at BSO concentrations greater than 1.4 mM, in the NADH:BSOR reaction, inhibition by BSO was observed in the presence of 960 μM BSO, at pH 8. The kinetic analysis indicates that, with *R. sphaeroides* BSO reductase, decreased $K_{m,app}$ for a substrate results in inhibition of activity at lower concentrations of that same substrate. An increase in the slope of the parallel lines obtained in the NADH:BSO reductase assays was also observed with increasing BSO concentrations, but, at 1.92 mM BSO, the slope of the Lineweaver−Burk plot ($K_{m,appNADH}$ = 394 μM, $V_{max,app}$ = 2.8 units) decreased, and at 3.84 mM BSO, it increased again, suggesting the presence of a secondary lower affinity binding site for NADH which was not observed with NADPH at the same concentrations of BSO. The second binding site observed with NADH may be due to the formation of the inactive NADH−BSO reductase complex. We did not detect the formation of the corresponding NADPH−BSO complex at the concentrations of BSO utilized in our assays.

The double competitive inhibition in a Ping Pong Bi−Bi mechanism results from both substrates forming dead-end complexes with the wrong enzyme form as illustrated below. NADPH (substrate A), with a K_m of 65 μM, reduces the enzyme but also forms a dead-end complex with enzyme form F, at high concentrations of NADPH ($K_{i,NADPH}$ = 900 μM). Then BSO (substrate B), with a K_m of 714 μM, binds to the reduced enzyme form F, and is reduced to biotin but also forms a dead end-complex with enzyme form E, at high concentrations ($K_{i,BSO}$ = 6.1 mM). (*16*). The putative second binding site observed with NADH may correspond to the binding site which leads to the formation of the dead-end complex.

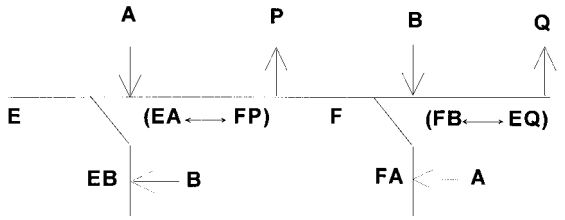

Slope replots of data obtained at high concentrations of the fixed substrate yielded a straight line and a K_i for BSO of 6.1 mM, a value which is very close to the value of 6.38 mM obtained using eq 1. The good agreement between these values supports the finding that BSO reductase from *R. sphaeroides* follows a Ping Pong Bi−Bi mechanism.

The Ping Pong mechanism may explain the relatively low substrate specificity of BSO reductase. It would be difficult to simultaneously accommodate two bulky substrates at the active site of this enzyme. In the Ping Pong mechanism, NADPH can bind, reduce the enzyme, and then dissociate. Following reduction of the enzyme, the second substrate can bind, with different affinities depending on the nature of the substrate, and is subsequently reduced.

The reversible inhibition of BSO reductase by cyanide supports recent studies on the active site of BSO reductase which indicated the absence of any sulfido ligands in the coordination sphere of the Mo atom and the presence of only four thiols donated by the two MGD cofactors and an oxo ligand donated by the side chain of a serine residue (Oγ) of the protein (*14*, *23*). In contrast, molybdoenzymes that have a terminal cyanolysable sulfur (S═O) bound as one of the ligands to Mo are irreversibly inactivated by treatment with cyanide due to the formation of thiocyanate. These inactivated enzymes can be reactivated only by chemical treatment with sulfide (*18*).

Recent EPR, XAS, and EXAFS studies to probe the active site of BSO reductase indicated that there are subtle but important differences in the dithionate- and NADPH-reduced forms of this enzyme (*23*). These differences may result from a direct hydride transfer to the Mo center following reduction with NADPH but not with dithionite. Our kinetic isotope effect studies on this enzyme strongly suggest that a hydride transfer (involving bond breaking) from NADPH to the enzyme occurs during the reduction of the enzyme by NADPH (*24*).

The X-ray crystal structure for the closely related enzyme, DMSO reductase has recently been determined to 3.5 Å resolution (*20*). The crystal structure indicates that, in DMSO reductase, there are three histidine residues involved in

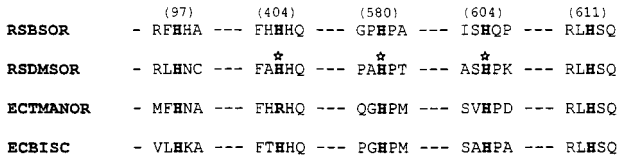

FIGURE 9: Conserved His residues in the DMSO reductase family of Mo-enzymes. The star (★) indicates the His residues shown to bind cofactor in the X-ray crystal structure of DMSO reductase, and the numbers in brackets indicate the actual position of that His residue in the amino acid sequence of the respective protein (*20*). RSBSOR represents *Rhodobacter sphaeroides* biotin sulfoxide reductase (*2*), RSDMSOR represents *Rhodobacter sphaeroides* dimethyl sulfoxide reductase (*23*), ECTMANOR represents *E. coli* trimethylamine N-oxide reductase (*24*), and ECBISC represents *E. coli* biotin sulfoxide reductase.

binding the MGD cofactor, H438, H643, and H649. Multiple alignments of amino acid sequences of the proteins comprising the DMSO reductase family, which include *R. sphaeroides* BSO and DMSO reductases and *E. coli* trimethylamine N-oxide reductase and BSO reductases, indicated that these three His residues are conserved in BSO reductase, as well as the remaining Mo-enzymes within the class that are characterized by the presence of a mono-oxo-Mo(VI) center, as shown in Figure 9. In addition to these cofactor-binding residues, there are also seven noncofactor-binding His residues which are also conserved between BSO and DMSO reductase. These observations prompted us to investigate the effect of DEPC-modification of BSO reductase. The decrease in NADPH:BSO reductase activity coupled with the loss of MGD cofactor clearly demonstrate that His residues are involved in cofactor binding in BSO reductase.

This work provides further insight into understanding the kinetic mechanism by which BSO reductase converts BSO to biotin. Although this enzyme is unique among Mo-enzymes, since it contains the Mo-cofactor as its sole prosthetic group and can also utilize NADPH directly, it still retains some features including cofactor binding, Mo coordination sphere, and broad substrate specificity which are common to most of the Mo-enzymes that comprise the DMSO reductase family.

REFERENCES

1. Pollock V. V., and Barber, M. J. (1995) *Arch. Biochem. Biophys. 318*, 322−332.
2. Pollock, V. V., and Barber, M. J. (1997) *J. Biol. Chem. 272*, 3355−3362.
3. Ejiri, S.-I., Weissbach, H., and Brot, N. (1980) *Anal. Biochem. 102*, 393−398.
4. Brot, N., Weissbach, L., Werth, J., and Weissbach, H. (1981) *Proc. Natl. Acad. Sci. U.S.A. 78*, 2155−2158.
5. Fridovich, I. (1989) *J. Biol. Chem. 264*, 7761−7764.
6. Pierson, D. E., and Campbell, A. (1990) *J. Bacteriol. 172*, 2194−2198.
7. del Campillo-Campbell, A. D., Dykhuizen, D., and Cleary, P. P. (1979) *Methods Enzymol. 62*, 379−385.
8. Laemmli, U. K. (1970) *Nature 227*, 680−685.
9. Jeong, S.-S., and Gready, J. E. (1994) *Anal. Bichem. 221*, 273−277.
10. Viola, R. E., Cook, P. F., and Cleland, W. W. (1979) *Anal. Chem. 96*, 334−340.
11. Trimboli, A. J., Quinn, G. B., Smith, E. T., and Barber, M. J. (1996) *Arch. Biochem. Biophys. 331*, 117−126.
12. Kletzin, A., and Adams, M, W. W. (1996) *FEMS Microbiol. Rev. 18*, 5−63.
13. Fromm, H. J. (1979) *Methods Enzymol. 63*, 42−53.
14. Garton, S. D., Temple, C. A., Dhawan, I. K., Barber, M. J., Rajagopalan, K. V., and Johnson, M. K. (2000) *J. Biol. Chem. 275*, 6798−6805.
15. Cleland, W. W. (1979) *Methods Enzymol. 63*, 500−513.
16. Segel, I. H. (1993) *Enzyme Kinetics: Behaviour and analysis of rapid equilibrium and steady-state enzyme systems*, pp 826−831, John Wiley and Sons, Inc., New York.
17. Schauer, N. L., and Ferry, J. G. (1986) *J. Bacteriol. 165*, 405−411.
18. Mitchell, P. C., and Pygall, C. F. (1979) *J. Inorg. Biochem. 11*, 25−29.
19. Hille, R. (1996) *SBIC 1*, 397−404.
20. Schindelin, H., Kisker, C., Hilton J., Rajagopalan, K. V., and Rees, D. C. (1996) *Science 272*, 1615−1621.
21. Barber, M. J., Van Valkenburg, H., Trimboli, A. J., Pollock, V. V., Neame, P. J., and Bastian, N. R. (1995) *Arch. Biochem. Biophys. 320*, 266−275.
22. Lundblad, R. L. (1995) *Techniques in protein modifications*, CRC Press Inc.
23. Temple, C. A., George, G. N., Hilton, G. C., George, M. J., Prince, R. C., Barber, M. J., and Rajagopalan, K. V. (2000) *Biochemistry 39*, 4046−4052.
24. Enemark, J. H., and Garner, C. D. (1997) *J. Biol. Inorg. Chem. 2*, 817−822.
25. Hilton J. C., and Rajagopalan K. V. (1996) *Biochem. Biophys Acta 1294*, 111−114.
26. Mejean, V., Iobbi-Nivol, C., Lepelletier, M., Giordano, G., Chippaux, M,, and Pascal, M. C. (1994) *Mol. Microbiol. 11*, 1169−1179.

BI001842D